Available online at www.sciencedirect.com
SCIENCE DIRECT®
ELSEVIER
Journal of Sound and Vibration 274 (2004) 1031–1044
JOURNAL OF SOUND AND VIBRATION
www.elsevier.com/locate/jsvi

On the non-linear dynamic behavior of a rotor–bearing system

Jing JianPing[a,*], Meng Guang[a], Sun Yi[b], Xia SongBo[b]

[a] *The State Key Laboratory of Vibration, Shock & Noise, ShangHai JiaoTong University, ShangHai, 200030, People's Republic of China*

[b] *Department of Astronautics and Mechanics, Harbin Institute of Technology, Harbin, 150001, People's Republic of China*

Received 31 January 2002; accepted 10 June 2003

Abstract

The non-linear dynamic behavior of a rotor–bearing system is analyzed based on a continuum model. The finite element method is adopted in the analysis. Emphasis is given on the so-called "oil whip phenomena" which might lead to the failure of the rotor system. The dynamic response of the system in an unbalanced condition is approached by the direct integration method and mode superposition method. It is found that a typical "oil whip phenomenon" is successfully produced. Furthermore, the bifurcation behavior of the oil whip phenomenon that is much concerned by present non-linear dynamics is analyzed. The rotor–bearing system is also examined by the simple discrete model. Significant differences are found between these two models. It is suggested that a careful examination should be made in modelling such non-linear dynamic behavior of the rotor system.

0. Introduction

Oil whip is a kind of self-exciting vibration of a rotor–bearing system and has brought about several destroying accidents in turbine generators since the 1970s [1]. Many studies have been conducted on oil whip by linear dynamics, but they cannot explain the phenomenon well. Presently, many efforts have been taken try to analyze the bifurcation behavior of oil whip by non-linear dynamics. But because the oil whip is difficult to produce by a non-linear mathematical model, the oil whip still cannot be explained by a non-linear dynamics phenomenon.

Rotor assembly is a complicated system. An accurate model may take into account many factors, such as mass, moment inertia, inner damping, bending and torsion vibration coupling effects, the non-linear factors of oil film bearing, and so on. In most studies, however, the

*Corresponding author.
E-mail address: jianpj@sjtu.edu.cn, jianpj@163.com (Jing JianPing).

0022-460X/$ - see front matter © 2003 Elsevier Ltd. All rights reserved.
doi:10.1016/S0022-460X(03)00663-1

non-linear dynamic behavior of rotor–bearing system was mainly approached by a simple discrete model [2,3]. The model has only very limited degrees of freedom and the influence of many factors (as mentioned above) was neglected. Such kinds of models may be adequate in determining the overall stable behavior of rotor systems. However, they might not be able to describe the complex non-linear dynamic behaviors after bifurcation. More elaborate models, such as continuum models, are therefore expected to provide better results. In the present study, a continuum model of rotor–bearing system is analyzed by the finite element method and the non-linear oil film force is taken into account. The non-linear dynamic behavior of the system is examined in detail and a typical "oil whip phenomenon" is produced. The results are then compared with the simple discrete model. It is found that there exists a significant difference between these two models. In fact, the "oil whip phenomenon" could hardly be reproduced by the simple discrete model, at least in the case of the present study. Therefore a careful examination is needed in modelling the non-linear dynamic behavior of the rotor system.

1. Model of non-linear rotor–bearing system

Consider a simple one-disk symmetric flexible rotor supported by two oil-lubricating bearings, as shown in Fig. 1. The dynamic behavior of the rotor is approached by the finite element method. The total rotor is divided into eight beam elements, and nine nodes; every node has four degrees of freedom including two rotating and two translation freedom. The masses of the disk and the bearing are treated as a lumped mass and are superimposed upon the corresponding nodes. The support of bearings is treated as a non-linear oil-film force applied to the ends of the rotor. The total finite element model is shown in Fig. 2.

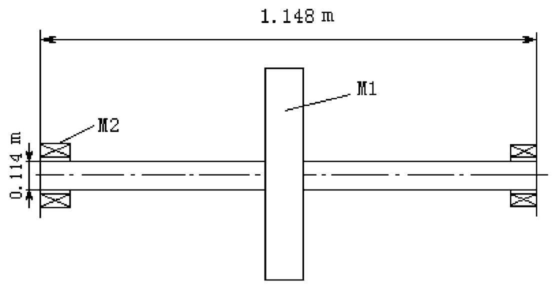

Fig. 1. A symmetric rotor–bearing system.

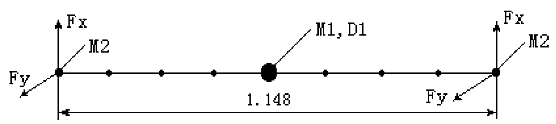

Fig. 2. Finite element model of the rotor–bearing system.

The oil-film force is obtained from short bearing theory and it can be expressed as [4,5]

$$\begin{Bmatrix} f_x \\ f_y \end{Bmatrix} = -\frac{[(x-2\dot{y})^2+(y+2\dot{x})^2]^{1/2}}{1-x^2-y^2}\begin{Bmatrix} 3xV(x,y,\alpha)-\sin\alpha G(x,y,\alpha)-2\cos\alpha S(x,y,\alpha) \\ 3yV(x,y,\alpha)+\cos\alpha G(x,y,\alpha)-2\sin\alpha S(x,y,\alpha) \end{Bmatrix}, \quad (1)$$

where x and y are planar co-ordinates of the axial center. The superposed dot denotes the time derivative of the variable:

$$V(x,y,\alpha)=\frac{2+(y\cos\alpha-x\sin\alpha)G(x,y,\alpha)}{1-x^2-y^2}, \quad (2)$$

$$S(x,y,\alpha)=\frac{x\cos\alpha+y\sin\alpha}{1-(x\cos\alpha+y\sin\alpha)^2}, \quad (3)$$

$$G(x,y,\alpha)=\frac{2}{(1-x^2-y^2)^{1/2}}\left[\frac{\pi}{2}+\operatorname{arctg}\frac{y\cos\alpha-x\sin\alpha}{(1-x^2-y^2)^{1/2}}\right], \quad (4)$$

$$\alpha=\operatorname{arctg}\frac{y+2\dot{x}}{x-2\dot{y}}-\frac{\pi}{2}\operatorname{sign}\left(\frac{y+2\dot{x}}{x-2\dot{y}}\right)-\frac{\pi}{2}\operatorname{sign}(y+2\dot{x}). \quad (5)$$

2. Integration method

Considering the non-linear lubricating force, the FEA dynamics equation of a non-linear rotor–bearing system can be expressed as

$$M\ddot{q}+D\dot{q}+Kq=R(\dot{q},q,\omega,t), \quad (6)$$

$$q_1=[x_1,\theta_{x1},\ldots,x_n,\theta_{xn}]^{\mathrm{T}},\ \ q_2=[y_1,\theta_{y1},\ldots,y_n,\theta_{yn}],$$

$$M=\begin{bmatrix} m & 0 \\ 0 & m \end{bmatrix},\quad q=\begin{Bmatrix} q_1 \\ q_2 \end{Bmatrix},\quad D=\begin{bmatrix} d & 0 \\ 0 & d \end{bmatrix},\quad [K]=\begin{bmatrix} K_x & 0 \\ 0 & K_y \end{bmatrix},\quad R=\begin{Bmatrix} R_1(\dot{q}_1,q_1,\omega,t) \\ R_2(\dot{q}_2,q_2,\omega,t) \end{Bmatrix},$$

$$d=\begin{bmatrix} \ddots & & \\ & D_1 & \\ & & \ddots \end{bmatrix}.$$

In Eq. (6), when the rotating speed changes, the eccentricity force will also change. Therefore, the responses of the rotor and the lubricating force will adjust to balance the eccentricity force. Changing ω, the non-linear responses of the rotor at different rotating speeds will be obtained.

Nowadays, Direct Integration method and Mode Superposition method are mainly used to solve Eqs. (6). Although Mode Superposition method has the advantage of saving calculation time, it may not be able to obtain accurate results when some modes are reduced. The Mode Superposition method is approached as follows:

From the vibration equation of the system without damping

$$[M]\{\ddot{q}\} + [K]\{q\} = 0. \tag{7}$$

The generalized eigenvalue problem can be obtained as

$$[K]\{\phi\} = \omega^2[M]\{\phi\}. \tag{8}$$

Solving Eq. (8), the m $(m \leqslant n)$ pairs of eigenvalues $(\omega_1^2, \{\phi_1\})$, $(\omega_2^2, \{\phi_2\})$, $\ldots$, $(\omega_m^2, \{\phi_m\})$ can be obtained. These eigenvectors $\{\phi_i\}$ $(i = 1, 2, \ldots, m)$ are orthogonal for $[M]$, i.e.

$$\{\phi_i\}^{\mathrm{T}}[M]\{\phi_j\} = \begin{cases} 1, & i = j, \\ 0, & i \neq j. \end{cases} \tag{9}$$

$\{\phi_i\}$ is called the ith mode vector, ω_i is the corresponding frequency of the mode.

For the eigenvector matrix $[\Phi]$ of Eq. (8) it can be deduced that

$$[K][\Phi] = [M][\Phi][\Omega]^2 \tag{10}$$

and $[\Phi] = [\{\phi_1\}\{\phi_2\}\cdots\{\phi_m\}]$, $[\Omega]^2 = \mathrm{diag}(\omega_1^2, \omega_2^2, \ldots, \omega_m^2)$

Due to

$$[\Phi]^{\mathrm{T}}[K][\Phi] = (\mathrm{diag}[\Omega])^2, \tag{11}$$

$$[\Phi]^{\mathrm{T}}[M][\Phi] = [I]. \tag{12}$$

Apparently, eigenvector matrix $[\Phi]$ is a good transform matrix, and it can transform the $[K]$ and $[M]$ into diagonal matrices with minimum bandwidth.

Therefore, it can be deduced that

$$\{q\} = [\Phi]\{\bar{X}\} \tag{13}$$

by substituting Eq. (13) into Eq. (6), it can be deduced

$$\{\ddot{\bar{X}}(t)\} + [\bar{D}]\{\dot{\bar{X}}(t)\} + [\Omega]^2\{\bar{X}(t)\} = \{\bar{R}(T)\}. \tag{14}$$

For an overall response, all the solutions of Eq. (14) must be calculated, and superpose the responses of every mode to obtain the displacements of the finite element nodes, i.e.

$$\{q(t)\} = \sum_{i=1}^{m} \{\phi_i\} z_i(t). \tag{15}$$

$\{\phi_i\}$ is ith mode vector, $z_i(t)$ is the general displacement and Eq. (15) is called the Mode Superposition method.

When the number of selected modes is less than the rank number of the nodes' displacement vector, the calculation of Eqs. (8) and (15) will be reduced. However, it is difficult to select a proper m for maintaining a good precision and also enhancing the solving efficiency.

There are three kinds of widely used Direct Integration methods, Center-Difference , Wilson-θ and Newmark method. Due to the fact that the Center-Difference method becomes stable only when some conditions are satisfied and the interval of solving time is difficult to choose, its application is restricted. Although the consumption of the calculation time for the Wilson-θ

and Newmark method are almost the same, the Newmark method has a higher accuracy than Wilson-θ [6]. Therefore, the Newmark method is adopted in solving the non-linear problem. The difference format of Newmark is

$$\{\dot{q}_{t+\Delta t}\} = \{\dot{q}_t\} + [(1-\delta)\{\ddot{q}_t\} + \delta\{\ddot{q}_{t+\Delta t}\}]\Delta t, \tag{16}$$

$$\{q_{t+\Delta t}\} = \{q_t\} + \{\dot{q}_t\}\Delta t + \left[\left(\frac{1}{2}-\alpha\right)\{\ddot{q}_t\} + \alpha\{\ddot{q}_{t+\Delta t}\}\right]\Delta t^2. \tag{17}$$

The parameters α and δ, are determined in terms of the precision and stability requirements of the integration. As $\delta = \frac{1}{2}$, $\alpha = \frac{1}{6}$, this method is correspondent to a Linear Acceleration method.

Considering the dynamics equation at $t + \Delta t$

$$[M]\{\ddot{q}_{t+\Delta t}\} + [D]\{\dot{q}_{t+\Delta t}\} + [K]\{q_{t+|\Delta t}\} = \{R_{t+\Delta t}\}. \tag{18}$$

Via Eq. (17), the $\{\ddot{q}_{t+\Delta t}\}$ can be calculated by $\{q_{t+\Delta t}\}$, then substitute $\{\ddot{q}_{t+\Delta t}\}$ into Eq. (16), and the equations of $\{\ddot{q}_{t+\Delta t}\}$ and $\{\dot{q}_{t+\Delta t}\}$ only written in $\{q_{t+\Delta t}\}$ can be obtained. Substituting these two equations of $\{\dot{q}_{t+\Delta t}\}$ and $\{\ddot{q}_{t+\Delta t}\}$ into Eq. (18), the $\{q_{t+\Delta t}\}$ can be calculated. Using Eqs. (16) and (17), $\{\dot{q}_{t+\Delta t}\}$ and $\{\ddot{q}_{t+\Delta t}\}$ can be obtained. The final equations are as follows:

$$\begin{aligned}
&\left([K] + \frac{1}{\alpha\Delta t^2}[M] + \frac{\delta}{\alpha\Delta t}[D]\right)\{q_{t+\Delta t}\} \\
&= [\hat{K}]\{q_{t+\Delta t}\} \\
&= \{R_{t+\Delta t}\} + [M]\left(\frac{1}{\alpha\Delta t^2}\{q_t\} + \frac{1}{\alpha\Delta t}\{\dot{q}_t\} + \left(\frac{1}{2\alpha}-1\right)\{\ddot{q}_t\}\right) \\
&\quad + [D]\left(\frac{\delta}{\alpha\Delta t}\{q_t\} + \left(\frac{\delta}{\alpha}-1\right)\{\dot{q}_t\} + \frac{\Delta t}{2}\left(\frac{\delta}{\alpha}-2\right)\{\ddot{q}_t\}\right) \\
&= \{\hat{R}_{t+\Delta t}\},
\end{aligned} \tag{19}$$

$$\{\ddot{q}_{t+\Delta t}\} = \frac{1}{\alpha\Delta t^2}(\{q_{t+\Delta t}\} - \{q_t\}) - \frac{1}{\alpha\Delta t}\{\dot{q}_t\} - \left(\frac{1}{2\alpha}-1\right)\{\ddot{q}_t\}, \tag{20}$$

$$\{\dot{q}_{t+\Delta t}\} = \{\dot{q}_t\} + (1-\delta)\Delta t\{\ddot{q}_t\} + \delta\Delta t\{\ddot{q}_{t+\Delta t}\}. \tag{21}$$

The above deduced process shows that

(1) The Newmark method is an implicit integration method.

(2) For the Newmark method, a special initial condition is not required, as the displacements, velocities and accelerations at $t + \Delta t$ are calculated only by the variables at t.

(3) It can be demonstrated that as $\delta \geqslant 0.5$ and $\alpha \geqslant 0.25\ (\delta + 0.5)^2$, the integration is absolutely stable. $\delta = 0.5$ and $\alpha = 0.25$ is often adopted.

(4) As the Newmark method is absolutely stable, it can be free of the trouble of choosing the time interval Δt. Due to the fact that equations must be calculated in every step, the Newmark method is more expensive than the Center-Difference method.

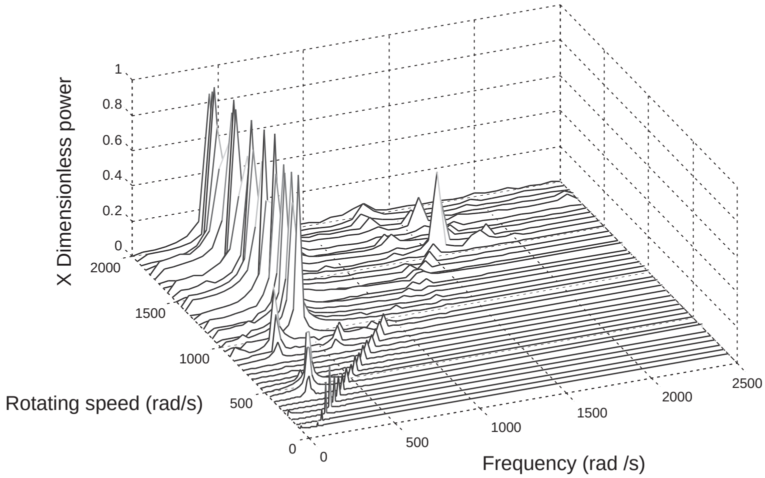

Fig. 3. Cascade spectrum of the vibrational responses of the rotor.

3. Numerical analysis and comparison of the non-linear dynamics of the rotor

For the mathematical model in Section 2, the parameters of the rotor and the bearing are chosen as $M_1 = 374$ kg, $M_2 = 27$ kg, $\mu = 18 \times 10^{-3}$ Pa s, $R = 57$ mm, $L = 28.5$ mm, $c = 0.2$ mm, $D_1 = 3.0 \times 10^3$ N s/m, and the eccentricity of the rotor is $\rho = 0.1$. In this section, the vibrational responses of the rotor in the speed-ascending process are studied and the cascade spectrum of the rotor vibrational response is given in Fig. 3. The overall bifurcation map is given in Fig. 4. All the above vibrational responses are calculated by the Newmark method.

The cascade spectrum of the vibrational response of the rotor exhibits the following dynamic phenomena.

(1) When the shaft rotates with a low rotating speed, there are only the synchronous (one per one rotation) vibrations with minor amplitudes (see Fig. 3). These vibrations are caused by the inertia forces of unbalance of the rotor.
(2) At higher rotation speeds, the forced synchronous vibration is not the only regime of motion. Along with synchronous vibrations, Oil Whirl appears (see Fig. 3). Oil whirl is the rotor lateral forward precessional subharmonic vibration around the bearing center. The amplitudes of oil whirl are much higher than those of synchronous vibrations;
(3) When the increasing rotation reaches the first balance resonance, i.e., the first natural frequency of the rotor, the oil whirl suddenly disappears.
(4) When the rotation speed approaches double the value of the rotor first balance resonance, the half-speed oil whirl frequency reaches the value of the first balance resonance—the first natural frequency of the rotor. The oil whirl pattern becomes replaced by Oil Whip—a lateral forward precessional subharmonic vibration of the rotor. Oil whip has a constant frequency: independent of the rotation speed increase, the oil whip frequency remains close to the first natural frequency of the rotor, and the amplitudes of oil whip are much higher than those of synchronous vibrations and oil whirl.

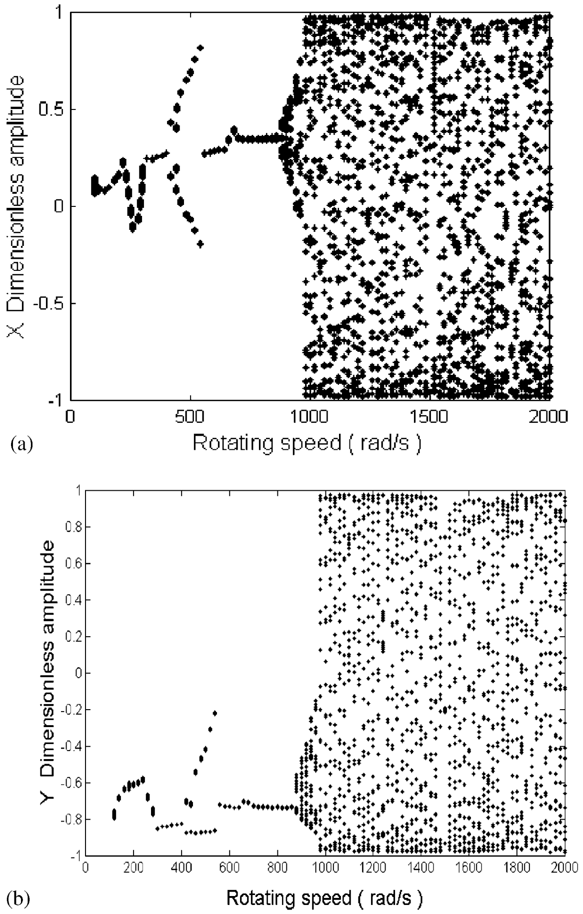

Fig. 4. Bifurcation behaviour of the rotor: (a) Bifurcation of x-response of shaft center at bearing. (b) Bifurcation of y-response of shaft center at bearing.

In order to demonstrate the oil whip phenomenon, the vibrational responses of the rotor system in the speed-descending process are also calculated. The amplitudes of the rotor in the speed-descending and speed-ascending processes are given in Fig. 5. The results show that in the speed-descending process, the oil whip does not disappear just at the point where it took place in the speed-ascending process until the speed descends to a lower speed. This is a typical characteristic of oil whip [7,8].

The bifurcation map of the rotor response shows that when the rotation speed reaches about $\omega = 500$ rad/s, a typical period-doubling bifurcation takes place, and then the responses become synchronous vibration. When the rotation speed reaches near $\omega = 900$ rad/s, the vibrations become quasi-period bifurcation. Therefore, the oil whirl and oil whip process is a typical Hopf bifurcation with hysteresis [9,10]. This result is very useful in the non-linear design of rotor–bearing system. The vibrational responses of rotor at several rotating speeds are also given in Figs. 6–8.

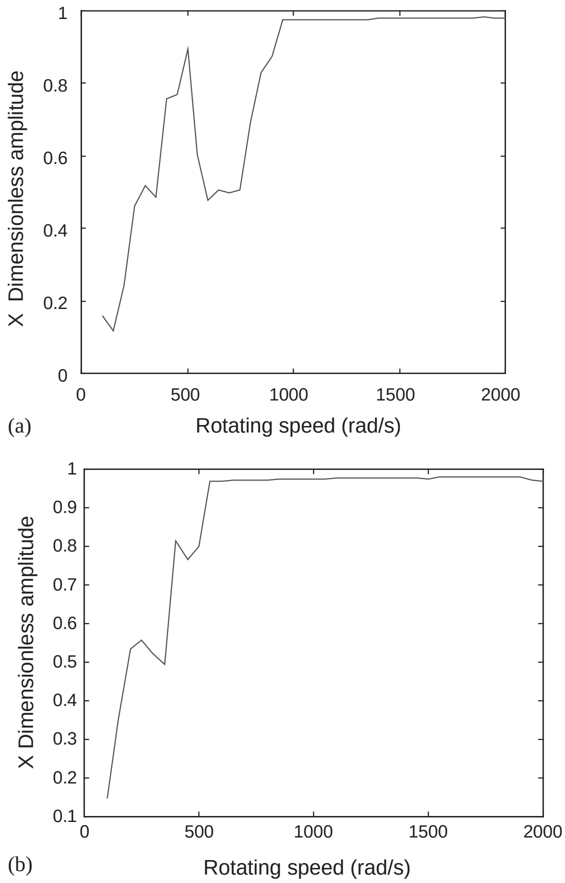

Fig. 5. Amplitudes of the rotor in the speed ascending and descending process: (a) Amplitudes of the rotor in the speed ascending process. (b) Amplitudes of the rotor in the speed descending process.

In order to check the difference between the Mode Superstition method and Direct Integration method, the dynamic responses of the rotor at the speed of $\omega = 600\,\mathrm{rad/s}$ are studied by these two methods, respectively, and the trajectories of the rotor are shown in Fig. 9. The trajectories of the rotor from the two methods show that the reduction of modes will bring about error in the solution and the more the modes are reduced, the more the error is brought in. In the calculation process, we also find that the solution of the oil-film force is apt to overflow due to the error from the mode reduction. The results show that the Direct Integration method is more effective and practical than the Superstition method in the calculation of the non-linear dynamic response.

At present, the non-linear dynamic behaviors of such kinds of rotors are mostly calculated by a simple discrete method. In order to study the differences of the solution between these two methods, the non-linear vibrational responses of the rotor (shown in Fig. 1) are calculated by the discrete method. The total rotor–bearing system is simplified into three mass points and the masses of the shaft are contributed to these three points. The stiffness of the two segments of the rotor is equivalent to k_p.

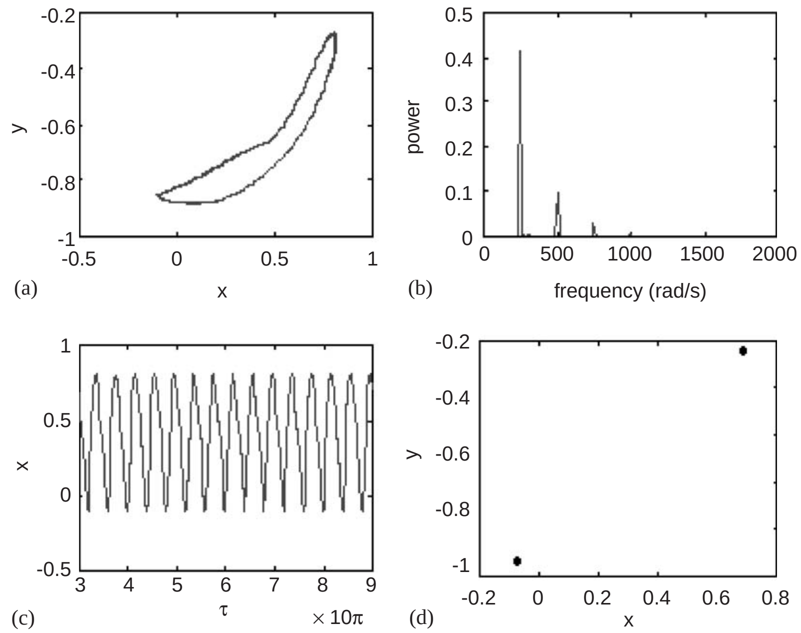

Fig. 6. Responses of the rotor ($\omega = 500$ rad/s): (a) trajectory in xy plane; (b) spectrum of frequency; (c) x motion versus τ; (d) Poincaré mapping.

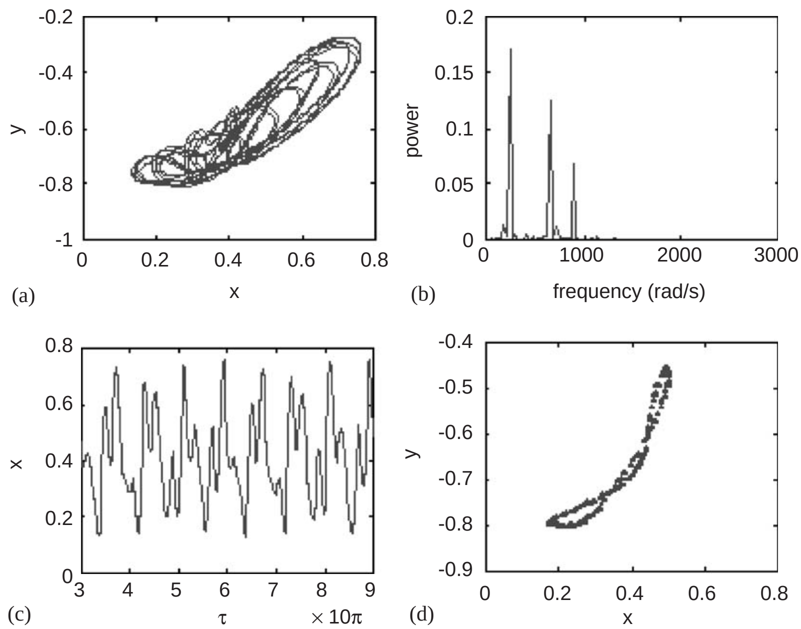

Fig. 7. Responses of the rotor ($\omega = 900$ rad/s): (a) trajectory in xy plane; (b) spectrum of frequency; (c) x motion versus τ; (d) Poincaré mapping.

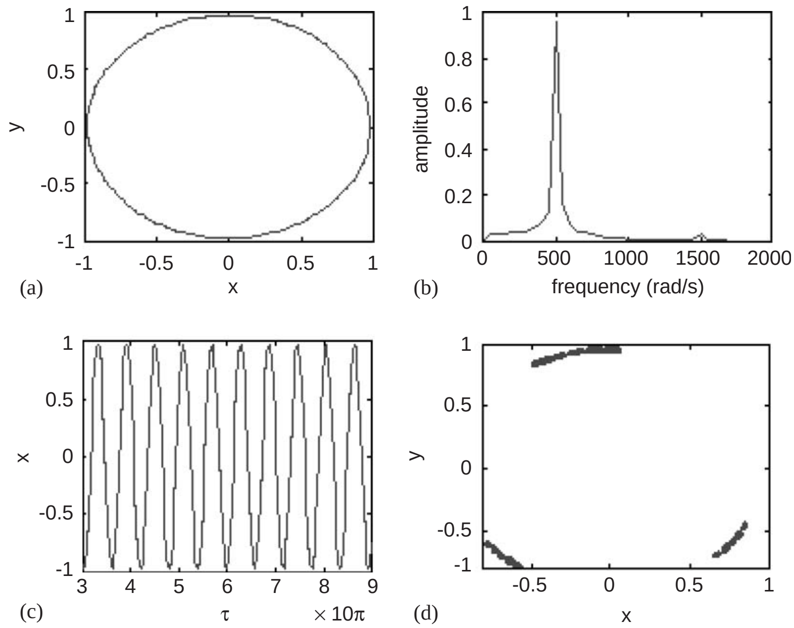

Fig. 8. Responses of the rotor ($\omega = 1500$ rad/s): (a) trajectory in xy plane; (b) spectrum of frequency; (c) x motion versus τ; (d) Poincaré mapping.

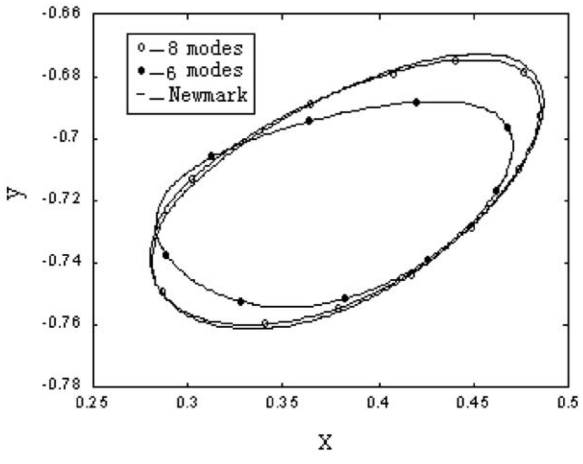

Fig. 9. Comparison of the results of Newmark and Mode Superposition scheme ($\omega = 600$ rad/s).

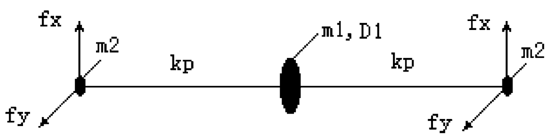

Fig. 10. Discrete mathematical model of the rotor.

The damping of the disk is D_1, and the lubricating force is loaded on the mass points corresponding to the bearings. The mathematical model is shown in Fig. 10, and the dynamic equations of the model are expressed as

$$\begin{cases} \ddot{x}_2 = -\dfrac{k}{m_2}(x_2 - x_1) + \dfrac{1}{m_{22}} f_x, \\ \ddot{y}_2 = -\dfrac{k}{m_2}(y_2 - y_1) + \dfrac{1}{m_{22}} f_y - G, \\ \ddot{x}_1 = -\dfrac{a}{m_1}\dot{x}_1 - \dfrac{2k}{m_1}(x_1 - x_2) + \rho\cos\tau, \\ \ddot{y}_1 = -\dfrac{a}{m_1}\dot{y}_1 - \dfrac{2k}{m_1}(y_1 - y_2) + \rho\sin\tau - G. \end{cases} \tag{22}$$

The parameters of the rotor are $m_1 = 420$ kg, $m_2 = 50$ kg, $2k_p = 2.105e + 8$ N/m, $D_1 = 3.0 \times 10^3$ N s/m. The parameters of the lubrication bearing are the same as those in the finite element model. By employing the Runge–Kutta scheme, the bifurcation behaviors of the rotor at the eccentricity of $\rho = 0.1$ are calculated and shown in Fig. 11. The bifurcation behaviors are quite

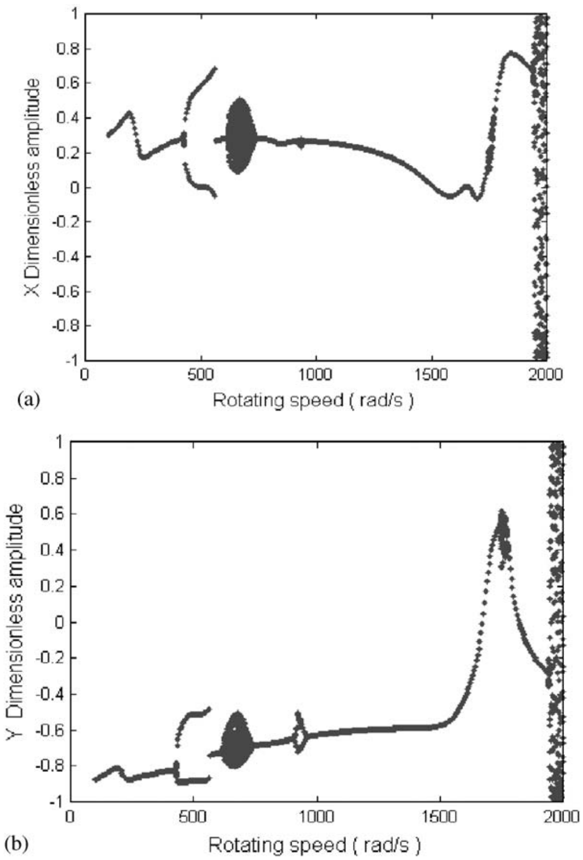

Fig. 11. Bifurcation behaviour of the rotor responses from Discrete model: (a) Bifurcation of x-response of shaft center at bearing. (b) Bifurcation of y-response of shaft center at bearing.

different from those from the finite element method. Due to the neglect of the effects of mass distribution and other inner non-linear factors, the solutions from the simple discrete method will deflect from the facts of the continuum rotor–bearing systems' non-linear vibrations.

4. Conclusions

In this paper, a continuum rotor–bearing system is modelled by finite element and the vibrational responses are calculated by employing Newmark and Mode Superposition schemes. The results are also compared with those from the discrete method, and the conclusions drawn from the study can be summarized as follows:

(1) The comparison of the results from the Newmark and Mode Superposition method shows that the mode reduction will bring about error in the solution of rotor's non-linear vibrational responses. The more the modes are reduced, the more the error occurs. In the calculation process, we also find that the solution of the oil-film force is apt to overflow due to the error from the mode reduction. The results show that the Direct Integration method is more accurate and practical than the Superstition method in the calculation of the non-linear dynamic response.
(2) Due to the neglect of the effects of mass distribution and other inner non-linear factors, the solutions from simple discrete method will deflect from the facts of the continuous rotor–bearing system's non-linear vibration. It cannot describe the non-linear vibrational behavior of a continuous rotor system correctly. While, the finite element method can take into account the effects of multi factors, the results from the finite element method will be more accurate than those from the simple discrete method.
(4) The vibrational responses of the rotor in the present study show that Oil Whirl and Oil Whip may take place in the speed descending process, and from the view of non-linear dynamics, it is a Hopf bifurcation, and they should be avoided in the design of this kind of rotor.

Acknowledgements

The project was supported by China "863" Project (No. 2002AA412410) and China Post doctoral Science Foundation.

Appendix. Nomenclature

M general mass matrix
m component mass matrix
D damping matrix
K stiff matrix
$\{R\}$ load tensor
$\{\ddot{q}\}$ acceleration tensor

$\{\dot{q}\}$ velocity tensor
$\{q\}$ displacement tensor
M_1 mass of disk
M_2 mass of bearing
D_1 damping coefficient of disk
δ sommerfeld modifying parameter ($\delta = \mu\omega RL(R/c)^2(L/2R)^2$)
μ viscosity of lubricating oil
c clearance of bearing radius
L length of bearing
R radius of bearing
F_x lubricating force in x direction ($F_x = f_x \cdot \delta$)
F_y lubricating force in y direction ($F_y = f_y \cdot \delta$)
f_x dimensionless lubricating force in x direction
f_y dimensionless lubricating force in y direction
ω rotating speed of rotor
t time
X displacement in x direction
Y displacement in y direction
x dimensionless displacement in x direction ($x = X/c$)
y dimensionless displacement in y direction ($y = Y/c$)
$\dot{x}$ dimensionless velocity in x direction
$\dot{y}$ dimensionless velocity in y direction
$\ddot{x}$ dimensionless acceleration in x direction
$\ddot{y}$ dimensionless acceleration in y direction
G dimensionless weight ($G = g/c\omega^2$)
τ dimensionless time ($\tau = \omega t$)
e eccentricity of rotor
ρ dimensionless eccentricity of rotor
m_1 lumped mass of bearing and part of shaft section
m_2 lumped mass of disk and part of shaft section
k_p effective stiffness of half shaft
k modified stiffness ($k = k_p/\omega^2$)
a modified damping ($a = D_1/\omega$)
m_{22} modified mass ($m_{22} = m_2\omega^2 c/\delta$)

References

[1] X.Y. Zhang, et al., On site testing and analysis of the oil whirl and oil whip phenomena in national-made 200MW steam turbine generator systems, *Power Industry* 12 (5) (1992) 32–37.
[2] P. Sundarajan, S.T. Noah, An algorithm for response and stability of large order nonlinear systems—application to rotor system, *Journal of Sound and Vibration* 214 (4) (1998) 695–723.
[3] T.S. Zheng, On stability and bifurcation analysis of high-dimensional rotor-bearing systems with local nonlinearity, *Acta Aeronautics* 19 (3) (1997) 284–292 (in Chinese).

[4] G. Adiletta, A.R. Guido, C. Rossi, Chaotic motions of a rigid rotor in short journal bearings, *Nonlinear Dynamics* 10 (1996) 251–269.

[5] G. Adiletta, et al., Nonlinear dynamics of a rigid unbalanced rotor in journal bearings. Part I: theoretical analysis, *Nonlinear Dynamics* 14 (1997) 57–87.

[6] J.Y. He, X.D. Lin, *Numerical Solution Methods of Nonlinear Problems in Engineering Structures*, National Defense Publisher, Beijing 1994, pp. 208–219.

[7] A. Muszynska, Whirl and whip-rotor/bearing stability problems, *Journal of Sound and Vibration* 110 (3) (1986) 443–462.

[8] A. Muszynska, Stability of whirl and whip in rotor/bearing system, *Journal of Sound and Vibration* 127 (1) (1988) 49–64.

[9] N.Sri. Namachchivaya, S.T. Ariaratnam, Stochastically perturbed Hopf bifurcations, *International Journal of Nonlinear Mechanics* 22 (5) (1987) 363–372.

[10] N.Sri. Namachchivaya, Hopf bifurcations in the presence of both parametric and external stochastically excitations, *Journal of Applied Mechanics* 55 (1988) 123–131.